Summary: In the present contribution, the electrostatic spinning or electrospinning technique was used to produce ultrafine polyamide-6 (PA-6) fibers. The effects of solution conditions on the morphological appearance and the average diameter of as-spun fibers were investigated by optical scanning (OS) and scanning electron microscopy (SEM) techniques. It was shown that the solution properties (i.e. viscosity, surface tension and conductivity) were important factors characterizing the morphology of the fibers obtained. Among these three properties, solution viscosity was found to have the greatest effect. Solutions with high enough viscosities (viz. solutions at high concentrations) were necessary to produce fibers without beads. At a given concentration, fibers obtained from PA-6 of higher molecular weights appeared to be larger in diameter, but it was observed that the average diameters of the fibers from PA-6 of different molecular weights had a common relationship with the solution viscosities which could be approximated by an exponential growth equation. Raising the temperature of the solution during spinning resulted in the reduction of the fiber diameters with higher deposition rate, while mixing *m*-cresol with formic acid to serve as a mixed solvent for PA-6 caused the solutions to have higher viscosities which resulted in larger fiber diameters. Lastly, the addition of some inorganic salts resulted in an increase in the solution conductivity, which caused the fiber diameters to increase due to the large increase in the mass flow.

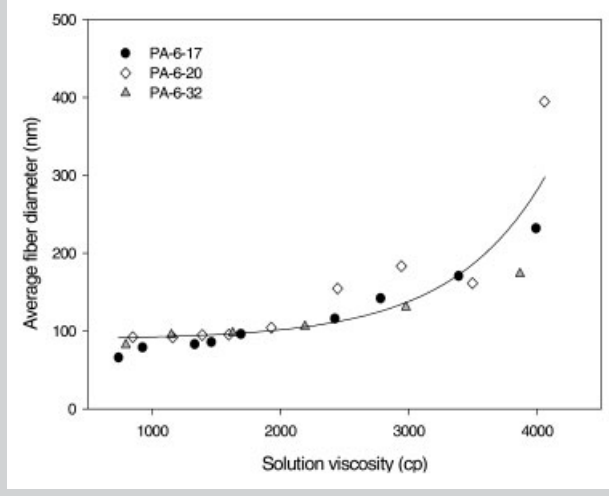

Average diameter of as-spun fibers plotted as a function of the viscosity of the solutions.

Ultrafine Electrospun Polyamide-6 Fibers: Effect of Solution Conditions on Morphology and Average Fiber Diameter

Chidchanok Mit-uppatham,[a] *Manit Nithitanakul, Pitt Supaphol**

The Petroleum and Petrochemical College, Chulalongkorn University, Soi Chula 12, Phyathai Road, Pathumwan, Bangkok 10330, Thailand
E-mail: pitt.s@chula.ac.th

Received: May 30, 2004; Revised: July 29, 2004; Accepted: August 30, 2004; DOI: 10.1002/macp.200400225

Keywords: electrospinning; fibers; polyamides

Introduction

High electrostatic fields have wide applications in many industries.[1] High electrostatic fields can be applied to either polymer solutions or melts to produce non-woven webs of ultrafine fibers, the diameters of which are in the range of few nanometers to sub-micrometers.[2–6] Such a technique is called electrostatic spinning or electrospinning. Due to the exceptionally high surface area to mass ratio of the fibers obtained and the high density of pores on the sub-micrometer length scale of the obtained non-woven webs, proposed applications for electrospun products are in areas where these properties are fully utilized. Some of the proposed applications for these products are as filters for the separation of sub-micron particles, as reinforcing fillers in composite materials, as wound-dressing and tissue scaffolding materials for medical uses and as controlled release materials for agricultural and pharmaceutical uses.[7]

The setup of the electrospinning process is very simple. The three major components are a high-voltage power

[a] On study leave from Department of Materials Technology, Faculty of Science, Ramkhamhaeng University, Bangkok 10240, Thailand.

supply, a container for a polymer solution or melt with a small opening to be used as a nozzle and a conductive collection device. An emitting electrode of the high-voltage power supply charges the polymer solution or melt by either directly submerging the electrode in the polymer solution or melt or by connecting the electrode to a conductive nozzle. The other or grounding electrode of the high-voltage power supply is connected to the conductive collection device to complete the circuit. Other setups are also possible.[7] The Coulombic repulsion force between charges of the same polarity produced in the polymer solution or melt by the emitting electrode destabilizes the hemi-spherical droplet of the polymer solution or melt located at the tip of the nozzle to finally form a droplet with a conical shape (i.e. the Taylor cone). With further increase in the electrostatic field strength beyond a critical value, the Coulombic repulsion force finally exceeds that of the surface tension which results in the ejection of an electrically charged stream of the polymer solution or melt (the charged jet).

There are six major forces acting on an infinitesimal segment of the charged jet. They are 1) body or gravitational forces, 2) electrostatic forces which carry the charged jet from the nozzle to the target, 3) Coulombic repulsion forces which try to push apart adjacent charged species present within the jet segment and are responsible for the stretching of the charged jet during its flight to the target, 4) viscoelastic forces which try to prevent the charged jet from being stretched, 5) surface tension which also acts against the stretching of the surface of the charged jet and 6) drag forces from the friction between the charged jet and the surrounding air.[8] Due to the combination of these forces, the electrically charged jet travels in a straight trajectory for only a short distance before undergoing a bending instability, which results in the formation of a looping trajectory.[9,10] During its flight to the collector, the charged jet thins down and, at the same time, dries out or solidifies to leave ultrafine fibers on the collective screen.

In the electrospinning process of a polymer solution, a number of parameters can influence the morphology of the obtained fibers. These governing parameters can be categorized into three main types: 1) solution (e.g. concentration, viscosity, surface tension and conductivity of the polymer solution), 2) process (e.g. applied electrostatic potential, collection distance and feed rate) and 3) ambient parameters (e.g. temperature, relative humidity and velocity of the surrounding air in the spinning chamber).[7,11] Baumgarten[12] was one of the early researchers who recognized the effects of some of these parameters on the morphological appearance of as-spun acrylic fibers. He found that an increase in the solution viscosity (as the result of an increase in the solution concentration) was responsible for an increase in the average fiber diameter, while an increase in the flow rate of the acrylic solution did not appreciably affect the fiber diameters.[12]

Fong and co-workers[13] investigated the formation of minute beads along electrospun poly(ethylene oxide) (PEO) fibers by relating the phenomenon to the properties of the solutions. They found that the number of beads decreased with increasing viscosity and net charge density, while it decreased with decreasing surface tension coefficient of the solutions.[13] Deitzel and co-workers[14] studied the effects of accelerating voltage and solution concentration on the morphological appearance of electrospun PEO fibers. Buchko and co-workers[15] found that the morphology of electrospun protein non-woven webs depended on solution concentration, applied electric field strength, deposition distance and deposition time. Demir and co-workers[16] found that the average diameter of electrospun fibers from polyurethaneurea copolymer increased with the third power of the solution concentration. Zong and co-workers[17] found that solution concentration and addition of ionic salts had stronger effects on the morphological appearance of electrospun poly(D,L-lactic acid) (PDLA) and poly(L-lactic acid) (PLLA) fibers than other parameters. Choices of solvent or a combination of solvents used were also found to have a significant effect on the morphology of the electrospun fibers.[8,18,19]

Although it has been shown in a recent review by Huang and co-workers[7] that various aspects of electrospun fibers have been intensely explored and reported in the open literature in the past, a number of fundamental aspects of the process for different polymer-solvent systems are still worthy of further investigation in order to gain a thorough understanding of the process. In the present contribution, the effects of various solution conditions (i.e. concentration, viscosity, surface tension, solution temperature, average molecular weight of the polymer and addition of ionic salt) on morphological characteristics of electrospun polyamide-6 (PA-6) fibers were investigated using optical scanning (OS) and scanning electron microscopy (SEM) techniques.

Experimental Part

Preparation and Characterization of Polyamide-6 Solutions

Three fiber spinning grades of polyamide-6 (PA-6) (AFC-2002, AFC-2001 and AFC-3003) were supplied by Asia Fiber Public Co., Ltd. (Thailand). The weight-average molecular weights for these resins were reported to be 17 000, 20 000 and 32 000 Da, respectively. From this point forward, these resins will be called PA-6-17, PA-6-20 and PA-6-32, respectively. Solutions for electrospinning were prepared by dissolving each resin in a specified amount in formic acid (85% v/v, Carlo Erba). Slight stirring was used to expedite dissolution. Solutions of varying concentrations (10 to 46% w/v for PA-6-17 and PA-6-20 resins and 10 to 34% w/v for PA-6-32 resin) were used to elucidate the effects of solution concentration and the average molecular weight of PA-6 on the morphological appearance of the obtained fibers. Various ionic salts (NaCl, LiCl and $MgCl_2$) in various amounts were added to a PA-6 solution of specified

concentration in order to investigate the effect of ionic salt addition on the morphological appearance of the as-spun fibers. The effect of the solvent system on the obtained fibers was studied by using a mixture of formic acid and *m*-cresol in various volumetric ratios to prepare PA-6 solutions. A Brookfield DV-III programmable viscometer, a Krüss K10T tensiometer and a Orion 160 conductivity meter were respectively used to measure viscosity, surface tension and conductivity of the as-prepared solutions at room temperature (ca. 30 °C) prior to electrospinning.

Setup of Electrospinning Process

A 50 ml glass syringe was used to stock each of the as-prepared PA-6 solutions. A 1 cm long stainless steel needle (gauge number 26), with a blunt tip, was used as a nozzle. Both the syringe and the nozzle were tilted at approximately 10° from a horizontal baseline in order to maintain a hemispherical droplet at the tip of the nozzle. The feed rate of the PA-6 solutions was controlled by pressurized nitrogen gas through a flow meter. A piece of thick aluminium (Al) sheet was used as a collective screen. A Gamma High Voltage Research ES30P power supply was used to charge the spinning PA-6 solutions by connecting the emitting electrode of positive polarity to the nozzle and the grounding electrode to the collective screen. The distance between the tip of the nozzle and the collective screen defined a collection distance. In this particular work, a fixed electrostatic DC potential of 21 kV was applied over a fixed collection distance of 10 cm. Normally, the spinning solutions were kept at room temperature (i.e. 30 °C), but, in order to study the effect of solution temperature on the morphological appearance of the as-spun fibers, solutions at an elevated temperature (40, 50 or 60 °C) were prepared by using a home-made double-chambered syringe, in which the outer chamber was circulated with warm water of a specified temperature.

Characterization of As-Spun PA-6 Fibers

The morphological appearance of the as-spun PA-6 fibers was investigated visually from optical scanning photographs of the as-spun webs collected on Al sheets using a 1200CS BearPaw optical scanner (OS) and from scanning electron micrographs of a small section of the same webs using a JEOL JSM-4200 scanning electron microscope (SEM). The specimens for SEM observation were prepared by cutting an Al sheet covered with the as-spun webs and the cut section was carefully affixed to an SEM stub. Each specimen was gold-coated using a JEOL JFC-1100E sputtering device before being observed under the SEM. For each spinning condition, at least 80 measurements for the fiber diameter were recorded. Statistical analysis of the data obtained was carried out by constructing a histogram, from which an arithmetic mean and a standard deviation were obtained and reported.

Results and Discussion

Effect of PA-6 Concentration on Physical Properties of As-Prepared Solutions

Solutions of all PA-6 resins in 85% v/v formic acid were prepared at various concentrations, ranging from 10 to 46% w/v for PA-6-17 and PA-6-20 and from 10 to 34% w/v for PA-6-32. The maximum of 34 wt.-% for PA-6-32 was attained because the solutions prepared at higher concentrations were too viscous. Figure 1 shows the viscosity, surface tension and conductivity values for solutions of PA-6 resins in 85% v/v formic acid as a function of PA-6 concentration. The viscosity values for solutions of all PA-6 resins were found to increase with increasing PA-6 concentration, with the values for PA-6-32 being much greater than those for PA-6-17 and PA-6-20 which, at a given concentration, were found to be very comparable to each other. Specifically, the values for PA-6-17 and PA-6-20 were found to monotonically increase from ca. 40 cp at 10% w/v to ca. 4 000 cp at 46% w/v, while the value for PA-6-32 was found to monotonically increase from ca. 40 cp at 10% w/v to ca. 7 000 cp at 34% w/v (see Figure 1a). The relationship between the solution viscosity and the solution concentration for all PA-6 resins could be approximated with an exponential growth equation (see equations in Figure 1a). The selection of the exponential growth equation to describe the data was based solely on the quality of the fitting that the equation provided.

The surface tension values for solutions of all PA-6 resins were found to monotonically increase but only slightly with increasing PA-6 concentration. Specifically, the values for all of the solutions investigated were found to range between ca. 42 and 45 $mN \cdot m^{-1}$ (see Figure 1b). The conductivity values for solutions of all PA-6 resins were found to initially increase, reaching a maximum at a concentration of around 16 to 18% w/v and then decreased with any further increase in the concentration of the solutions. Specifically, the values for all of the solutions studied ranged between ca. 3.3 and 4.6 $mS \cdot cm^{-1}$. The results obtained illustrate that an increase in the PA-6 concentration resulted in a significant increase in the viscosity, a slight increase in the surface tension and a slight decrease in the conductivity of the resulting solution. The viscosity of the resulting solution increased appreciably with increasing molecular weight of the dissolved polymer, while both the surface tension and the conductivity values were relatively less affected. The significant increase in the viscosity of the solutions with increasing PA-6 concentration is obviously due to the increased molecular entanglements.

Effect of PA-6 Concentration

Figure 2 shows a selected series of scanning electron micrographs in order to illustrate the effect of the concentration of PA-6-17 solutions on the morphological appearance of the obtained as-spun materials. At low concentrations (from 10 to ca. 18% w/v) or low viscosities (39.2 to 157 cp), a large number of sub-micron droplets were present (see Figure 2a). At such low viscosities, the viscoelastic force (a result of the low degree of chain entanglements) in a given jet segment was not large enough to counter the higher Coulombic

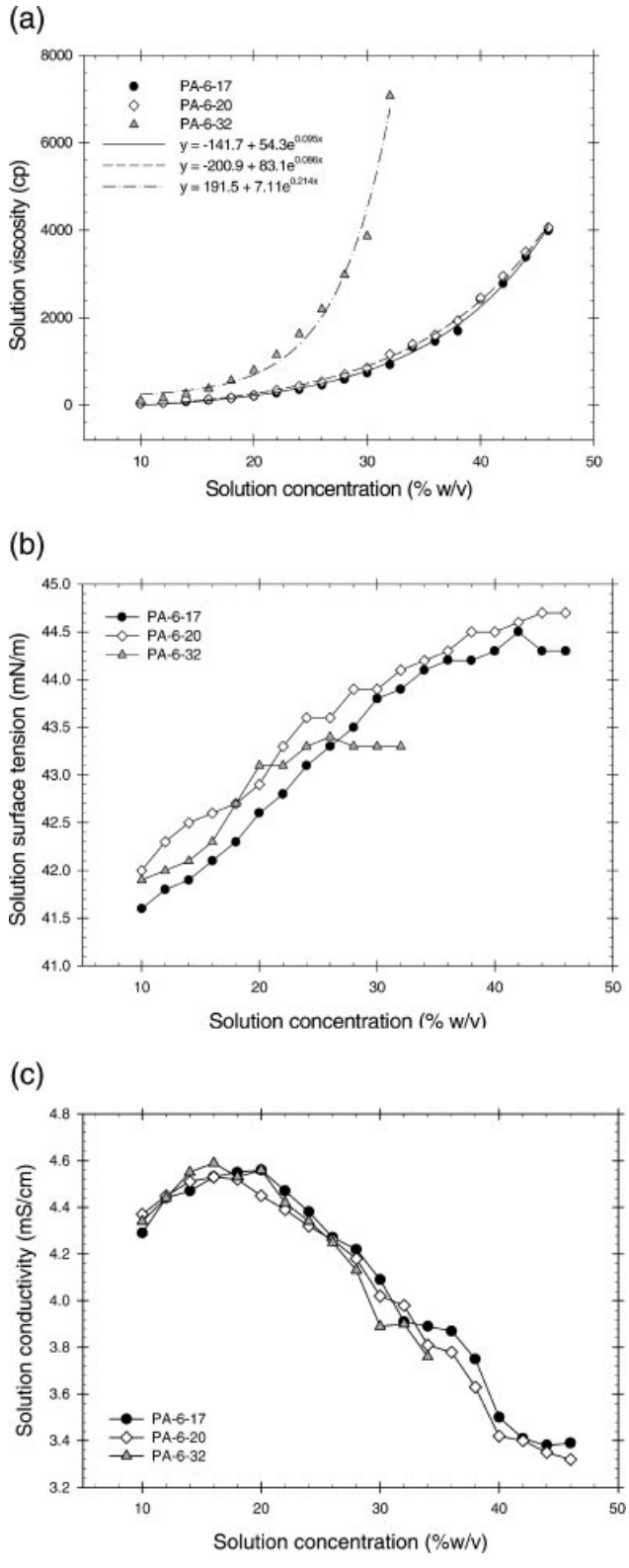

Figure 1. (a) Viscosity, (b) surface tension and (c) conductivity as a function of polyamide-6 concentration for solutions of polyamide-6 of three different weight-average molecular weights in 85% v/v formic acid.

force, resulting in the break-up of the charged jet into smaller jets, which, as a result of the surface tension, were later rounded up to form droplets. This phenomenon has been familiarized in industry as the electrospraying process and has commonly been used in many applications such as paint spraying, ink-jet printing and powder coating.[1]

At higher concentrations or higher viscosities, the charged jet did not break up into small droplets, a direct result of the increased chain entanglements (and hence an increase in the viscoelastic force) which were sufficient to prevent the break-up of the charged jet and to allow the Coulombic stress to further elongate the charged jet during its flight to the grounded target, which ultimately thinned down the diameter of the charged jet.[15] However, if the concentration was not high enough (e.g. 20% w/v), a combination of smooth fibers and minute, discrete droplets was obtained (see Figure 2b). A slight increase in the concentration of the solution to 22% w/v (or the viscosity to 277 cp) resulted in the disappearance of the minute, discrete droplets, leaving only a combination of smooth and beaded fibers on the target. With any further increase in the concentration (or viscosity) of the solution, the number of beads along the fibers was found to decrease and their shape appeared to be more elongated (see Figure 2c and d). When the concentration of the solution was increased to 34% w/v (or the viscosity to 1 332 cp), the beads disappeared altogether, leaving only smooth ultrafine fibers on the target.

The formation of beads along the as-spun fibers could be a result of a number of different phenomena. For example, it could be a result of the viscoelastic relaxation and the work of the surface tension upon the reduction of the Coulombic force once the fibers are in contact with the grounded target that drives the formation of the beads.[13] This phenomenon would only occur when the charged jet was not ''dry'' enough prior to its deposition on the target, causing some parts of the partially discharged jet to contract and form beads. As soon as the collected jet is ''dry'' enough, contraction can no longer occur any longer, thus leaving only beaded fibers on the target. The ''dryness'' of the charged jet is controlled mainly by the amount of solvent that can evaporate during the flight of the charged jet to the target. The amount of evaporating solvent is determined by a number of factors: the boiling point of the solvent, the initial concentration of the solution, the solution and the ambient temperatures, the diameter of the charged jet which continuously decreases during its flight to the target and the total path length that the charged jet travels from the nozzle to the target which significantly depends on the extent of the bending instability[9,10] that occurs.

The fact that beads along the fibers were observed at a concentration of 22% w/v and, with further increasing the concentration of the solutions to 34% w/v, the amount of beads decreased and the beads appeared to be more elongated in shape supports the above-mentioned postulation on the formation of beads. With increasing concentration

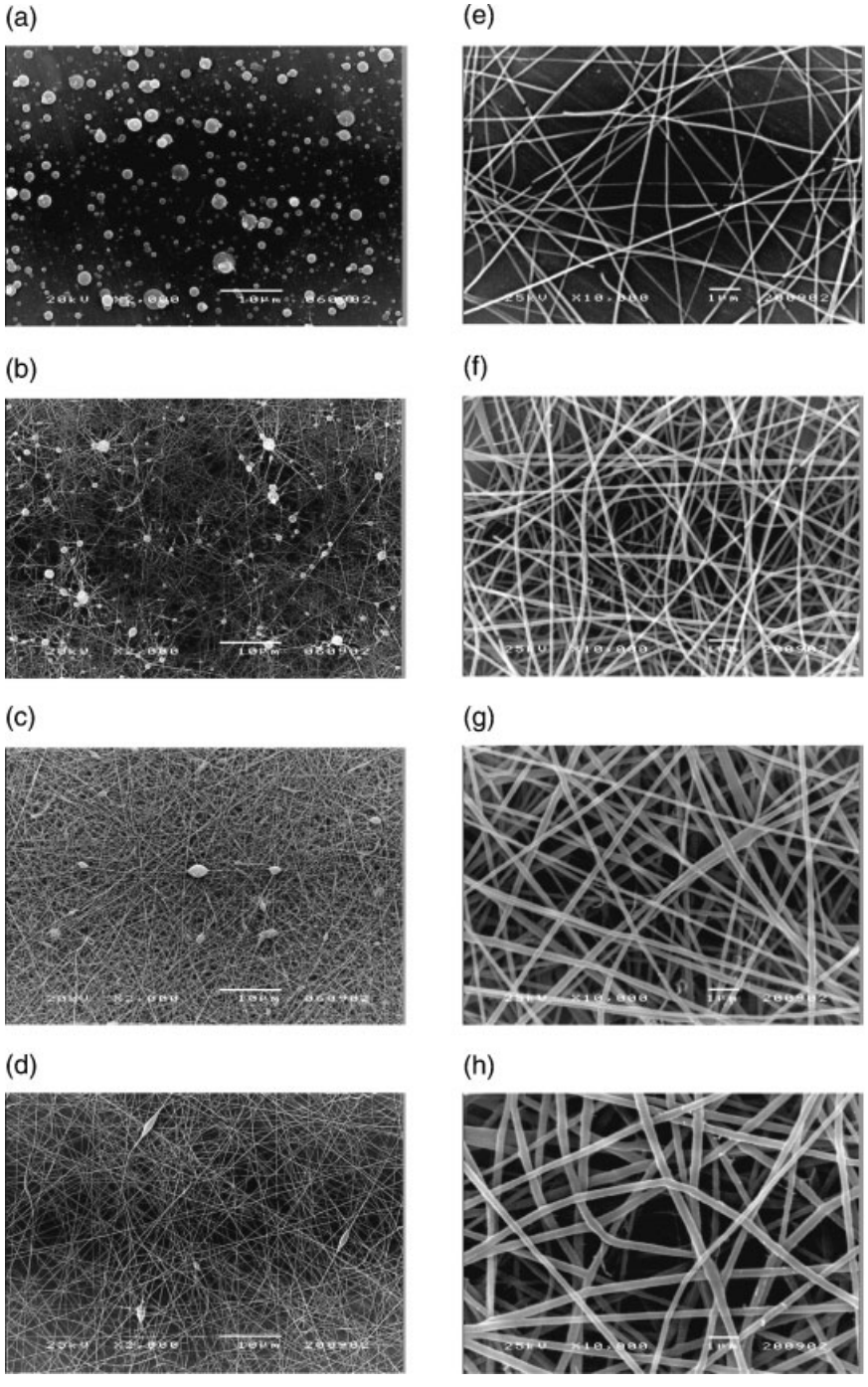

Figure 2. Scanning electron micrographs of electrospun materials obtained from solutions of PA-6-17 in 85% v/v formic acid at concentrations of a) 14, b) 20, c) 24 and d) 32% w/v (magnification = 2 000×, scale bar = 10 μm) and at concentrations of e) 32, f) 38, g) 42 and h) 46% w/v (magnification = 10 000×, scale bar = 1 μm).

(within the range 22 to 34% w/v), the initial amount of solvent in a small segment of a charged jet decreased, rendering the charged jet able to ''dry'' much more easily. However, the increased concentration enabled the charged jet to withstand a larger stretching force (from the Coulombic repulsion), resulting in the observed larger diameter of the charged jet (ultimately, the as-spun fibers). In addition, the observed larger diameter had an adverse effect on the extent of the bending instability which determined the total path length of a jet segment during its flight to the grounded

target. It should be noted that the longer path length means a higher probability for the jet segment to thin down as a result of the Coulombic repulsion.

Figure 3 illustrates the appearance of non-woven PA-6-17 webs on the grounded target. The concentrations of the solutions were 30, 38, 42 and 46% w/v, respectively, while the applied electrostatic field and the collection time were fixed at 21 kV/10 cm and 30 s, respectively. Obviously, the diameter of the non-woven webs obtained decreased, while the areal density of the obtained fibers increased, with increasing solution concentration. Due to an increase in the viscosity, the ejected, charged jet from solutions of higher concentrations had greater resistance towards the thinning of its diameter. This caused the charged jet to travel along a straight trajectory for a longer distance before undergoing a bending instability[9,10] and this is postulated to be the main reason for the observed smaller diameter of the non-woven webs collected at higher concentrations (see Figure 3). The observed longer distance of the straight trajectory with increasing concentration of PA-6-17 is in excellent agreement with an earlier report in a previous work[20] on poly(2-hydroxyethyl methacrylate) and polystyrene. Both the increase in the viscoelastic force and the decrease in the total path length of a jet segment resulted in an increase in the diameter of the as-spun fibers obtained from solutions of higher concentrations (see Figure 2e–h).

In order to quantitatively illustrate the effect of solution concentration on the diameters of the ultrafine PA-6-17 fibers, as-spun fibers with a small amount of beads present or no beads at all were measured for their diameter. The concentration of the solutions that resulted in such fibers was in the range of 30 to 46% w/v (equivalent to viscosity in the range 738 to 3 992 cp). Selected micrographs of some of these fibers are shown in Figure 2e–h at a magnification of 10 000×. Obviously from these micrographs, the diameters of the obtained fibers were found to increase with increasing solution concentration, as previously mentioned. Figure 4 shows plots of the average diameter of the as-spun fibers from solutions of PA-6-17 of various concentrations ranging from 30 to 46% w/v as a function of the solution concentration and the solution viscosity. Apparently, the average fiber diameter was found to increase monotonically from

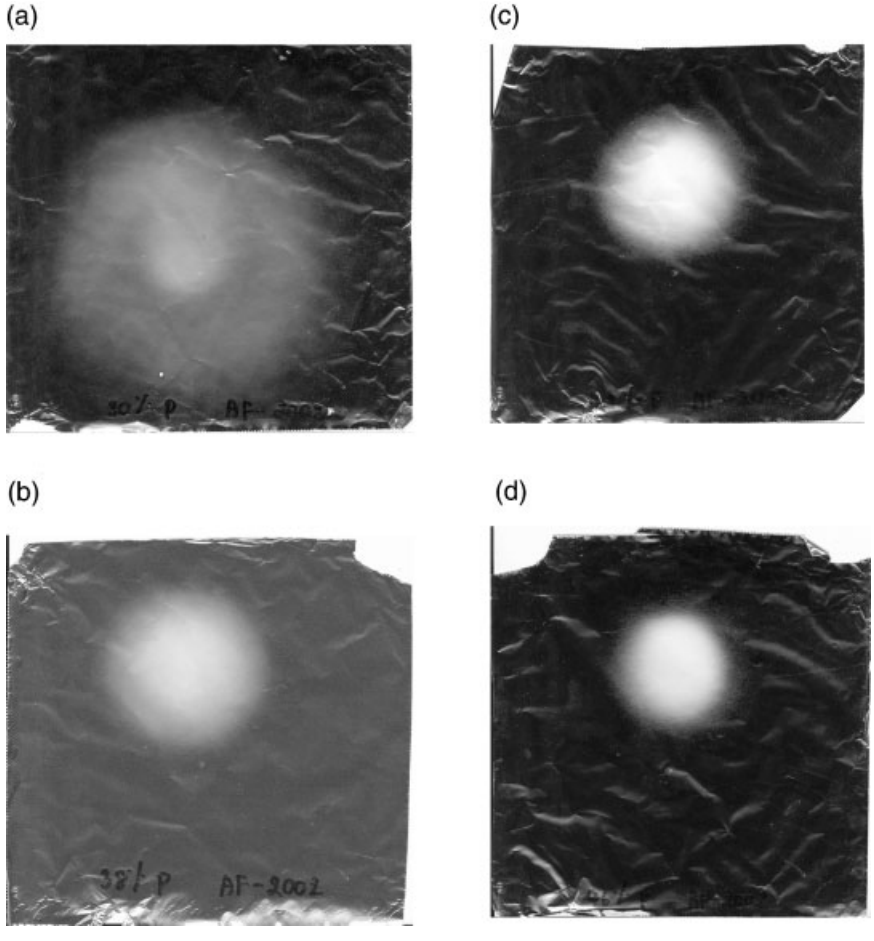

Figure 3. Optical scanning photographs of non-woven web of polyamide-6 fibers from solutions of PA-6-17 in 85% v/v formic acid at concentrations of 32, 38, 42 and 46% w/v. The collection time was fixed at 30 s.

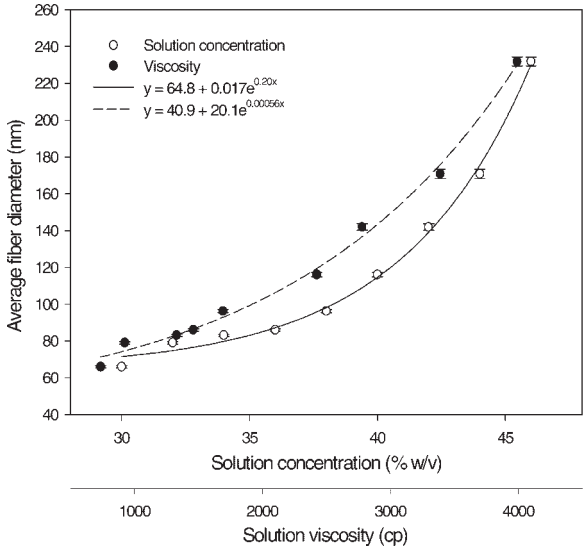

Figure 4. Average diameter of as-spun PA-6-17 fibers plotted as a function of the concentration and the viscosity of the solutions.

ca. 66 nm at 30% w/v (equivalent to a viscosity of 738 cp) to ca. 232 nm at 46% w/v (equivalent to a viscosity of 3 992 cp). Other studies found the average diameter of the as-spun PA-6 to be in the range 100–500 nm.[21,22] According to Figure 4, it was found that the relationships between the average fiber diameter and the solution concentration and between the average fiber diameter and the solution viscosity could be best described by an exponential growth equation (see equations in Figure 4). It should be noted here again that the selection of the exponential growth equation to describe the data was based solely on the quality of the fitting that the equation provided.

Effect of PA-6 Average Molecular Weight

Figure 5 shows a selected series of scanning electron micrographs portraying the effect of the average molecular weight of PA-6 on the morphological appearance of the as-spun materials obtained from three solutions of different concentrations (10, 20 and 34% w/v). Obviously, at 10% w/v,

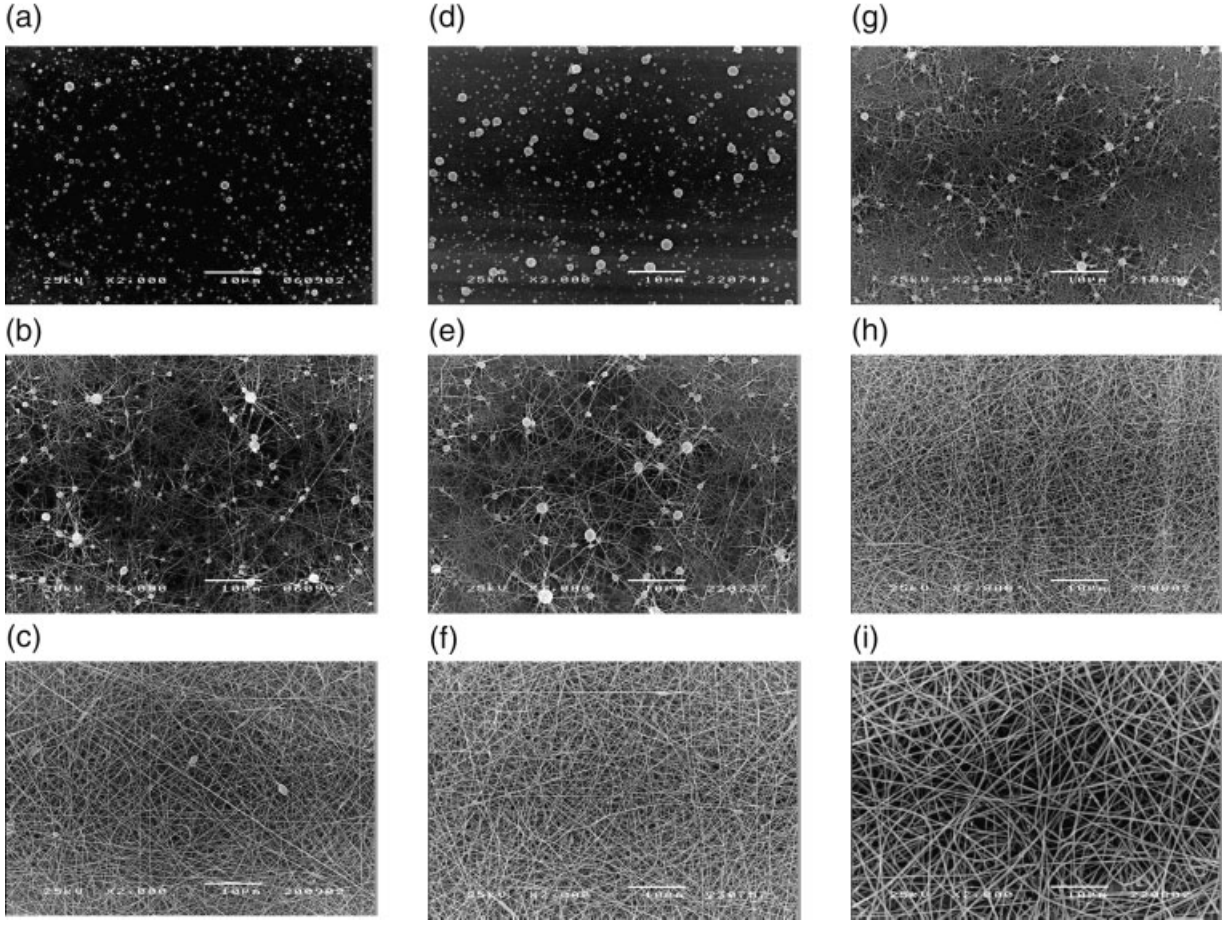

Figure 5. Scanning electron micrographs of electrospun materials obtained from solutions of PA-6-17 in 85% v/v formic acid at concentrations of a) 10, b) 20 and c) 34% w/v, from solutions of PA-6-20 in 85% v/v formic acid at concentrations of d) 10, e) 20 and f) 34% w/v, and from solutions of PA-6-32 in 85% v/v formic acid at concentrations of g) 10, h) 20 and i) 34% w/v (magnification = 2 000×, scale bar = 10 μm).

a large number of small droplets were present in the micrographs for PA-6-17 and PA-6-20 (see Figure 5a and d), while a mixture of small droplets and smooth fibers was obtained for PA-6-32 (see Figure 5g). At 20% w/v, a mixture of small droplets and smooth fibers was present in the micrographs for PA-6-17 and PA-6-20 (see Figure 5b and e), while only smooth fibers were observed in the case of PA-6-32 (see Figure 5h). By further increasing the solution concentration to 30% w/v, only smooth fibers were observed for all of the PA-6 resins investigated (see Figure 5c, f and i). It is apparent, based on the micrographs shown in Figure 5, that, for a given PA-6 resin, the tendency for the observation of droplets or beaded fibers was found to decrease, while the diameters of the smooth fibers obtained were found to increase with increasing solution concentration. The most likely explanation for such an observation is the much greater increase in the viscoelastic force as a result of the large increase in the degree of chain entanglements (due to the increase in the solution concentration and hence the increase in the solution viscosity) in comparison with the Coulombic force.

The critical concentrations for the observation of beaded fibers (in combination with some smooth fibers but without the presence of discrete droplets) and of smooth fibers (without the presence of beaded fibers) for the three resins were quite different. Specifically, the critical concentration for the observation of beaded fibers for PA-6-17 was 22% w/v, for PA-6-20 was 20% w/v and for PA-6-32 was 14% w/v, while the critical concentration for the observation of smooth fibers for PA-6-17 was 34% w/v, for PA-6-20 was 34% w/v and for PA-6-32 was 22% w/v. Interestingly, despite the difference in these critical concentrations, the critical viscosities for the observation of beaded fibers and of smooth fibers for the three resins were quite comparable. Particularly, the critical concentration for the observation of beaded fibers for PA-6-17 was 277 cp, for PA-6-20 was 225 cp and for PA-6-32 was 256 cp, while the critical concentration for the observation of smooth fibers for PA-6-17 was 1 332 cp, for PA-6-20 was 1 390 cp and for PA-6-32 was 1 150 cp. Based on the results obtained, the most important parameter determining the morphological appearance of the electrospun fibers was viscosity, rather than the concentration of the solution.

Figure 6 illustrates the average diameter of as-spun PA-6-17, PA-6-20 and PA-6-32 fibers plotted as a function of both the concentration and the viscosity of the solutions. It should be noted that the diameters of the obtained fibers were measured from micrographs showing the as-spun fibers with a small amount of beads present or no beads at all. In both PA-6-17 and PA-6-20, the measurable concentration of the solutions was in the range 30 to 46% w/v (equivalent to a viscosity in the range of 738 to 3 992 cp for PA-6-17 and of 849 to 4 058 cp for PA-6-20), while, in PA-6-32, the measurable concentration range was from 20 to 30% w/v (equivalent to a viscosity in the range of 795 to

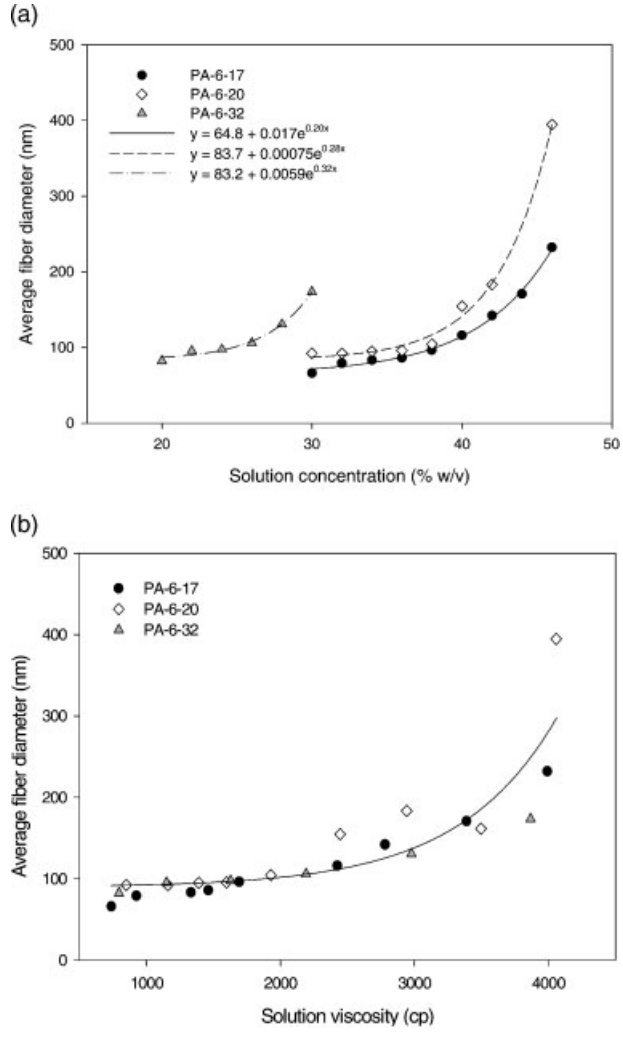

Figure 6. Average diameter of as-spun PA-6-17, PA-6-20 and PA-6-32 fibers plotted as a function of (a) the concentration and (b) the viscosity of the solutions.

3 867 cp). For a given PA-6 resin, the average fiber diameter was found to monotonically increase when increasing both the concentration and the viscosity of the solutions. Specifically, the average fiber diameter for PA-6-17 was found to increase from ca. 66 to 232 nm, for PA-6-20 from ca. 92 to 395 nm and for PA-6-32 from ca. 82 to 174 nm. It was also shown in Figure 6a that the average fiber diameter obtained for each resin exhibited a finite relationship with the solution concentration, which could be approximated by an exponential growth equation (see equations in Figure 6a).

Instead of plotting the average fiber diameter for each resin as a function of the solution concentration, the average fiber diameters for all of the resins were plotted as a function of the solution viscosity in Figure 6b. Apparently, the average fiber diameters for all of the resins exhibited a common relationship with the solution viscosity, especially within the viscosity range 738 to 2 191 cp. As was shown for the case of PA-6-17 resin in Figure 4, the common relationship

Table 1. Viscosity, surface tension and conductivity of 20% w/v polyamide-6 ($\overline{M}_w = 32\,000$ Da) solutions in 85% v/v formic acid at different temperatures and the diameter of the resulting as-spun fibers.

Solution temperature	Viscosity	Surface tension	Conductivity	Fiber diameter
°C	cp	$mN \cdot m^{-1}$	$mS \cdot cm^{-1}$	nm
30	517	43.2	4.2	98.3 ± 8.2
40	387	42.3	3.9	94.0 ± 6.3
50	284	41.8	3.8	91.8 ± 7.2
60	212	41.1	3.4	89.7 ± 5.6

between the average fiber diameters for all of the resins investigated and the respective solution viscosity could be numerically fitted to an exponential growth equation of the form:

$$\text{Average fiber diameter (nm)} = 88.7 + 0.804\exp(0.00137 \times \text{viscosity (cP)}) \quad (1)$$

Effect of Solution Temperature

In order to illustrate the effect of solution temperature on the morphological appearance of the as-spun PA-6 fibers, a solution of PA-6-32 in 85% v/v formic acid was prepared at a concentration of 20% w/v. Prior to electrospinning, the as-prepared solution was stocked in a home-made double-chambered syringe and its temperature was equilibrated by warm water, the temperature of which was set at 30, 40, 50 or 60 °C. Some physical properties (i.e. viscosity, surface tension and conductivity) of the as-prepared solution at the different temperatures investigated were measured and the results are summarized in Table 1. It should be noted that the viscosity and the surface tension of the solution measured at room temperature were 795 cp and 43.1 $mN \cdot m^{-1}$, respectively. According to Table 1, all of the solution property values were found to monotonically decrease with an increase in the solution temperature.

The as-spun PA-6-32 fibers obtained from the solutions at different temperatures were found to be similar in their morphology, which was a combination of beaded and smooth fibers. The only difference in the morphology of the fibers obtained was in the average fiber diameter, which was found to decrease from ca. 98 nm at a solution temperature of 30 °C to ca. 90 nm at a solution temperature of 60 °C (see Figure 7 for examples). Since the concentration of the solution was fixed, the elevation of the solution temperature resulted in the expansion of the polymer molecules, leading to a reduction in the degree of chain entanglements and hence a reduction in the solution viscosity. The reduction in the viscosity means there is a reduction in the viscoelastic

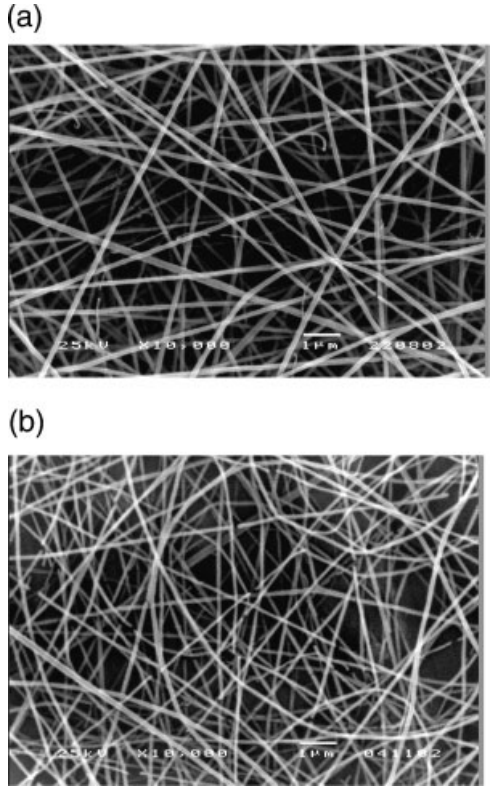

Figure 7. Scanning electron micrographs of electrospun fibers obtained from solutions of PA-6-32 at a concentration of 20% w/v in 85% v/v formic acid at solution temperatures of a) 30 and b) 60 °C (magnification = 10 000×, scale bar = 1 μm).

Table 2. Viscosity, surface tension and conductivity of 32% w/v polyamide-6 ($\overline{M}_w = 20\,000$ Da) solutions in a mixed solvent of 85% v/v formic acid and *m*-cresol in various compositional ratios (v/v) and the diameter of the resulting as-spun fibers.

Mixed solvent of formic acid and *m*-cresol in various compositional ratios	Viscosity	Surface tension	Conductivity	Fiber diameter
v/v	cp	$mN \cdot m^{-1}$	$mS \cdot cm^{-1}$	nm
100/0	1160	44.1	4.0	93.5 ± 6.0
90/10	1709	42.4	2.9	110.4 ± 6.9
80/20	2104	41.3	2.1	166.1 ± 10.5
70/30	3127	40.6	1.4	170.3 ± 9.8
60/40	4075	39.8	0.8	188.6 ± 17.3
50/50	4550	39.3	0.4	200.5 ± 13.2

force to counter the Coulombic stretching force, which finally results in the observed reduction in the fiber diameters.

Besides the reduction in the fiber diameters, the micrographs shown in Figure 7 also suggest that the number of fibers deposited on the target increased with increasing solution temperature. For a fixed mass throughput, the decrease in the average fiber diameter implied an increase in the total length of the as-spun fibers. For a fixed deposition period, the increase in the total length of the fibers resulted in an increase in the number of fibers deposited on the target. When working with the electrospinning of segmented polyurethaneurea (PUU) in dimethylformamide (DMF) at elevated temperatures of the solutions, Demir and coworkers[16] observed an increase in the deposition rate of the fibers as a function of the solution temperature, which is in agreement with the observations in this work.

Effect of Solvent System

In order to investigate the effect of the solvent system on the morphological appearance of the as-spun PA-6 fibers, solutions of PA-6-20 were prepared by dissolving the pellets in mixed solvents of 85% v/v formic acid and *m*-cresol in various compositional ratios between formic acid and *m*-cresol (90:10, 80:20, 70:30, 60:40 and 50:50 v/v) prior to electrospinning. Some physical properties (viscosity, surface tension and conductivity) of the as-prepared solutions were measured and the results are summarized in Table 2. It should be noted that the property values for the solution in 85% v/v formic acid were also listed for comparison. Interestingly, the viscosity of the solutions was found to markedly increase, the surface tension to decrease slightly and the conductivity to decrease appreciably with the addition and increasing amounts of *m*-cresol. The decrease in the conductivity of the solutions with increasing amounts of *m*-cresol could be a result of the much lower dielectric constant of *m*-cresol (11.5 at 23.9 °C[23]) in comparison with that of formic acid (58.5 at 15.6 °C[23]).

Figure 8 shows selected scanning electron micrographs of as-spun fibers obtained from the solutions of PA-6-20 in a mixed solvent of 85% v/v formic acid and *m*-cresol in various compositional ratios (90:10, 80:20 and 60:40 v/v). The micrograph exhibiting the as-spun fibers obtained from the solution of PA-6-20 in *m*-cresol is also shown for comparison (see Figure 8d). While the 32% w/v solution of PA-6-20 in 85% v/v formic acid produced smooth fibers, the 32% w/v solution of PA-6-20 in *m*-cresol produced nothing but blobs of solution on the collector. The most likely explanation for such an observation may be due to the much

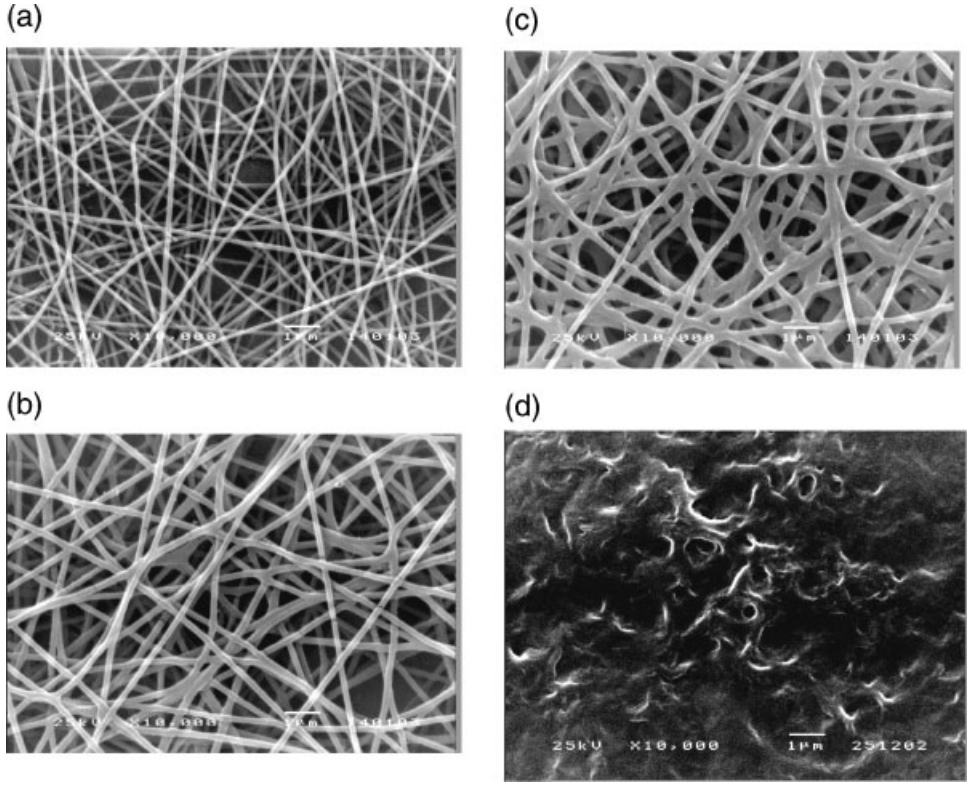

Figure 8. Scanning electron micrographs of electrospun fibers obtained from solutions of PA-6-20 at a concentration of 32% w/v in a mixed solvent of 85% v/v formic acid and *m*-cresol in various compositional ratios of a) 90:10, b) 80:20, c) 60:40 v/v and d) from a solution of PA-6-20 at a concentration of 32% w/v in *m*-cresol (magnification = 10 000×, scale bar = 1 μm).

higher boiling point of *m*-cresol (202 °C[24]) in comparison with that of formic acid (101 °C[25]). With such a high boiling point, the charged jet from the solution of PA-6-20 in *m*-cresol did not have enough time to ''dry'' prior to depositing on the target. The ''rather wet'' depositing jet then fused with adjacent depositing jets to form the blobs of solution observed.

In the mixed solvent system, smooth and separate fibers were obtained when the content of *m*-cresol was varied between 10 and 30% v/v and further increases in the *m*-cresol content to 40 and 50% v/v resulted in the observation of smooth fibers that were fused to one another at touching points (see Figure 8). The occurrence of the fused fiber morphology should be due to the high boiling point of *m*-cresol. Evidently, the diameters of the obtained fibers were found to increase with increasing the amount of *m*-cresol added. Specifically, the average fiber diameter increased from ca. 94 nm for PA-6-20 solution in 85% v/v formic acid to ca. 201 nm for PA-6-20 solution in a mixed solvent of 85% v/v formic acid and *m*-cresol at a compositional ratio of 50:50 v/v. The increase in the average fiber diameter with increasing *m*-cresol content could be due to both the increase in the solution viscosity and the decrease in the solution conductivity with increasing *m*-cresol content. This simply means that, at higher *m*-cresol contents, the Coulombic stretching force decreased, while the viscoelastic force which counters the Coulombic stretching force increased, resulting in an increase in the diameters of the as-spun fibers.

Effect of Salt Addition

In order to investigate the effect of salt addition on the morphological appearance of the obtained electrospun fibers, various types of inorganic salt (NaCl, LiCl and $MgCl_2$) in amounts ranging from 1 to 5% w/v were added to 32% w/v PA-6-20 solution in 85% v/v formic acid. The 5% w/v content of the inorganic salt was the dissolution limit for these salts in the 32% w/v PA-6-20 solution. Table 3 summarizes the viscosity, surface tension and conductivity values of the as-prepared solutions as well as the diameters of the obtained electrospun fibers. It should be noted that the viscosity, surface tension and conductivity values for the 32% w/v PA-6-20 solution in 85% v/v formic acid were ca. 1 160 cp, 44 $mN \cdot m^{-1}$ and 4 $mS \cdot cm^{-1}$, respectively. Obviously, the addition of these inorganic salts resulted in a marked reduction in the viscosity values and a marked increase in the conductivity values, although they seemed to not affect the surface tension of the obtained solutions.

According to Table 3, the viscosity values of PA-6-20 solutions with added NaCl or LiCl salts were found to increase with increasing salt content, while those of the solutions with added $MgCl_2$ seemed not to demonstrate a finite relationship with the salt content. In addition, the conductivity values of the solutions were found to increase monotonically with an increase in the salt content. For solutions containing NaCl and LiCl, the increase in the viscosity values suggests an increase in the viscoelastic force counteracting the Coulombic stretching force with increasing salt content, while, for all of the solutions investigated, the increase in the conductivity values suggests an increase in both the electrostatic and the Coulombic forces with increasing amounts of added salt. Intuitively, the increase in the Coulombic stretching force should result in a reduction in the obtained fiber diameters (provided that the viscoelastic force is more or less constant), but the results summarized in Table 3 suggest otherwise. The increase in the fiber diameters with increasing amounts of salt could be a result of the increase in the viscoelastic force (i.e. for fibers obtained from solutions containing NaCl and

Table 3. Viscosity, surface tension and conductivity of 32% w/v polyamide-6 ($\bar{M}_w = 20\,000$ Da) solutions in 85% v/v formic acid with the addition of NaCl, LiCl or $MgCl_2$ salt in various amounts ranging from 1 to 5% w/v and the diameter of the resulting as-spun fibers.

Type of salt added	Amount of salt added	Viscosity	Surface tension	Conductivity	Fiber diameter
	% w/v	cp	$mN \cdot m^{-1}$	$mS \cdot cm^{-1}$	nm
NaCl	1	558	43.5	6.2	98.6 ± 7.4
	2	576	43.9	8.0	101.5 ± 6.0
	3	599	44.0	9.6	114.3 ± 7.1
	4	556	44.9	11.1	124.8 ± 7.3
	5	694	44.9	12.2	134.2 ± 13.3
LiCl	1	614	43.8	6.3	105.4 ± 9.0
	2	683	43.9	8.5	138.2 ± 11.6
	3	708	43.8	10.3	147.8 ± 16.5
	4	783	44.3	11.9	168.7 ± 15.0
	5	871	45.0	13.1	168.3 ± 15.1
$MgCl_2$	1	639	43.8	5.0	99.4 ± 9.1
	2	644	43.9	5.8	102.7 ± 7.8
	3	604	44.1	6.5	118.8 ± 9.9
	4	618	44.1	7.2	127.7 ± 11.6
	5	634	44.2	8.3	131.7 ± 12.3

LiCl) and the increase in the mass flow (due to the increase in the electrostatic force acting on the jet segments). Demir and co-workers[16] also reported an increase in the mass flow with the addition of triethylbenzylammonium chloride to a solution of PUU in DMF.

Conclusion

In the present contribution, the effects of solution conditions on the morphological appearance and average diameter of as-spun polyamide-6 (PA-6) fibers were thoroughly investigated using optical scanning (OS) and scanning electron microscopy (SEM) techniques. An increase in the solution concentration caused a marked increase in the solution viscosity and the relationship between the solution viscosity and the solution concentration could be approximated by an exponential growth equation. At low solution viscosities, only small droplets were present. At slightly higher viscosities, a combination of small droplets and smooth fibers was obtained. At some critical viscosity, the droplets disappeared altogether, leaving only beaded and smooth fibers on the collective target. Further increasing the solution viscosity resulted in a reduced number of beads and increased fiber diameters. At high enough solution viscosities, only smooth fibers were present.

At a given concentration, fibers obtained from PA-6 of higher molecular weights appeared to be larger in diameter, but it was observed that the average diameters of the fibers obtained from PA-6 of different molecular weights exhibited a common relationship with the viscosities of the solutions which could be approximated by an exponential growth equation. An increase in the temperature of the solution during electrospinning resulted in a decrease in the fiber diameters, but resulted in an increase in the deposition rate. Mixing *m*-cresol with formic acid to serve as a mixed solvent for PA-6 caused the resulting solutions to have higher viscosity values which resulted in larger fiber diameters. Lastly, the addition of some inorganic salts to the solutions resulted in an increase in the conductivity values, which, in turn, caused the fiber diameters to increase due to the large increase in the mass flow.

Acknowledgements: The authors acknowledge partial support received from the *National Research Council of Thailand* (contract grant number: 03009582-0002), *Chulalongkorn University* (through invention and research grants from the Ratchadapesek Somphot Endowment Fund), the *Petroleum and Petrochemical Technology Consortium* [through a Thai governmental loan from the Asian Development Bank (ADB)], and the *Petroleum and Petrochemical College* (PPC), Chulalongkorn University. Helpful discussions with Dr. *Ratthapol Rangkupan* of the Metallurgy and Materials Science Research Institute (MMRI), Chulalongkorn University is also gratefully acknowledged.

[1] J. Cross, "*Electrostatics: Principles, Problems, and Applications*", Adam Hilger, Bristol 1987.
[2] US Patent 1,975,504 (1934), inv.: A. Formhals.
[3] US Patent 2,160,962 (1939), inv.: A. Formhals.
[4] US Patent 2,187,306 (1940), inv.: A. Formhals.
[5] US Patent 2,323,025 (1943), inv.: A. Formhals.
[6] US Patent 2,349,950 (1944), inv.: A. Formhals.
[7] Z. M. Huang, Y. Z. Zhang, M. Kotaki, S. Ramakrishna, *Compos. Sci. Technol.* **2003**, *63*, 2223.
[8] L. Wannatong, A. Sirivat, P. Supaphol, *Polym. Int.* **2004**, *53*, 1851.
[9] D. H. Reneker, I. Chun, *Nanotechnology* **1996**, *7*, 216.
[10] D. H. Reneker, A. L. Yarin, H. Fong, S. Koombhongse, *J. Appl. Phys.* **2000**, *87*, 4531.
[11] J. Doshi, D. H. Reneker, *J. Electrostat.* **1995**, *35*, 151.
[12] P. K. Baumgarten, *J. Colloid Interface Sci.* **1971**, *36*, 71.
[13] H. Fong, I. Chun, D. H. Reneker, *Polymer* **1999**, *40*, 4585.
[14] J. M. Deitzel, J. Kleinmeyer, D. Harris, N. C. Beck Tan, *Polymer* **2001**, *42*, 261.
[15] C. J. Buchko, L. C. Chen, Y. Shen, D. C. Martin, *Polymer* **1999**, *40*, 7397.
[16] M. M. Demir, I. Yilgor, E. Yilgor, B. Erman, *Polymer* **2002**, *43*, 3303.
[17] X. Zong, K. Kim, D. Fang, S. Ran, B. S. Hsiao, B. Chu, *Polymer* **2002**, *43*, 4403.
[18] H. Liu, Y. L. Hsieh, *J. Polym. Sci., Part B: Polym. Phys.* **2002**, *40*, 2119.
[19] K. H. Lee, H. Y. Kim, M. S. Khil, Y. M. Ra, D. R. Lee, *Polymer* **2003**, *44*, 1287.
[20] S. Koombhongse, Ph.D. thesis, University of Akron, Akron, Ohio 2001.
[21] X. Fang, Ph.D. thesis, University of Akron, Akron, Ohio 1997.
[22] H. Fong, W. Liu, C. Wang, R. Vaia, *Polymer* **2002**, *43*, 775.
[23] http://www.orioninstruments.com/html/dielectric_constants.asp.
[24] http://www.jtbaker.com/msds/englishhtml/c5456.htm.
[25] http://www.jtbaker.com/msds/englishhtml/f5956.htm.

